
On Catastrophic Forgetting and Mode Collapse in GANs

Hoang Thanh-Tung

Deakin University

Truyen Tran

Abstract

In this paper, we show that Generative Adversarial Networks (GANs) suffer from catastrophic forgetting even when they are trained to approximate a single target distribution. We show that GAN training is a continual learning problem in which the sequence of changing model distributions is the sequence of tasks to the discriminator. The level of mismatch between tasks in the sequence determines the level of forgetting. Catastrophic forgetting is interrelated to mode collapse and can make the training of GANs non-convergent. We investigate the landscape of the discriminator’s output in different variants of GANs and find that when a GAN converges to a good equilibrium, real training datapoints are wide local maxima of the discriminator. Catastrophic forgetting prevents the discriminator from making real datapoints its local maxima. Finally, we study methods for preventing catastrophic forgetting in GANs.

1 Introduction

GANs [1] are a powerful tool for modeling complex distributions. Training a GAN to approximate a single target distribution is often considered as a single task. In this paper, we introduce a novel view of GAN training as a continual learning problem in which the sequence of changing model distributions are considered as the sequence of tasks. We discover a surprising result that GANs suffer from catastrophic forgetting, a problem often observed in continual learning settings [2]. Catastrophic forgetting (CF) in artificial neural networks [3, 4, 5] is the problem where the knowledge of previously learned tasks is abruptly destroyed by

the learning of the current task. When a GAN suffers from CF, it exhibits undesired behaviors such as mode collapse and non-convergence.

In section 2, we show that GAN training is actually a continual learning problem and demonstrate the CF problem on a number of datasets. We show that catastrophic forgetting and mode collapse [1] are two different but interrelated problems and together, they can make the training of GANs non-convergent (section 2.2, 3.2). To avoid mode collapse and improve convergence, it is important to address the CF problem. We identify 2 factors that causes CF in GANs: 1) Information from previous tasks is not used in the current task, 2) Knowledge from previous tasks is not usable for the current task and vice versa. Our findings shed light on how to avoid catastrophic forgetting to learn the target distribution properly (Section 4).

In section 3, we investigate the effect of CF and mode collapse on the landscape of the discriminator’s output. We find that when a GAN converge to a good local equilibrium without mode collapse, real datapoints are wide local maxima of the discriminator. We show that the sharper the local maxima are, the more severe mode collapse is. Section 3.2 shows that when CF happen, the discriminator is directionally monotonic. A GAN with a directionally monotonic discriminator does not converge to an equilibrium. The fact confirms that CF is a cause of non-convergence.

Section 4 explains how state-of-the-art methods for stabilizing GANs such as Wasserstein GAN [6, 7], zero-centered gradient penalty on training examples (GAN-R1) [8], zero-centered gradient penalty on interpolated samples (GAN-0GP) [9], and optimizers with momentum, can prevent CF and mode collapse.

Contributions:

1. We detect the CF problem in GANs.
2. We show the relationship between CF, mode collapse, and non-convergence.
3. We study the relationship between the sharpness of local maxima and mode collapse.

4. We show that CF tends to make the discriminator directionally monotonic.
5. We identify the causes of CF and explain the effectiveness of methods for preventing CF in GANs.

2 Catastrophic forgetting problem in GANs

2.1 GAN training as a continual learning problem

Let us consider a GAN with generator $G(\cdot; \theta)$, a continuous function with parameter $\theta \in \mathbb{R}^m$; and discriminator $D(\cdot; \psi)$, a continuous function with parameter $\psi \in \mathbb{R}^n$. G transforms a d_z -dimensional noise distribution p_z to a d -dimensional model distribution p_g that approximates a d -dimensional target distribution p_r . D maps d -dimensional inputs to 1-dimensional outputs. Let \mathcal{L}_D be the loss function for D , \mathcal{L}_G be the loss function for G (Table 1). G and D are trained by alternating SGD.

At each iteration of the training process, G is updated to better fool D . p_g^t , the model distribution at iteration t , is different from the model distribution at the previous iteration p_g^{t-1} and the next iteration p_g^{t+1} . The knowledge required to separate p_g^t from p_r is different from that for the pair $\{p_g^{t-1}, p_r\}$. $\{p_g^{t-1}, p_r\}$ and $\{p_g^t, p_r\}$ are two different classification tasks to the discriminator.¹ The sequence of changing model distributions $\{p_g^i\}_{i=1}^T$ and the target distribution p_r form a sequence of tasks $\{\mathcal{T}^i = \{p_g^i, p_r\}\}_{i=1}^T$ to the discriminator. Because the generator at iteration t , G^t , can only generate samples from p_g^t , the discriminator at iteration t , D^t , cannot access samples from previous model distributions $p_g^i, i = 1, \dots, t-1$. That makes the learning process of D a continual learning problem. Similarly, the generator has to fool a sequence of changing discriminators $\{D^i\}_{i=1}^T$. The training process of a GAN poses a different continual learning problem to each of the players. In this paper, we focus on the continual learning problem in the discriminator as many prior works have showed that the quality of a GAN mainly depends on its discriminator [10, 11, 12].

If the sequence p_g^t converges to a distribution p_g^* , then the sequence of tasks $\{\mathcal{T}^i\}_{i=1}^T$ converges to a single task of separating 2 distributions p_g^* and p_r . In practice,

¹In the original theoretical formulation of GAN, at every GAN iteration, the discriminator and the generator are trained until convergence [1]. That means p_g^t can be arbitrarily different from p_g^{t-1} . In practice, however, at each iteration, only a limited number of gradient updates are applied to the players. We can consider a chunk of consecutive model distributions as a task to the discriminator.

however, the sequence of model distributions does not always converge. Nagarajan and Kolter [13] formally proved that the players in Wasserstein GAN [6] do not converge to an equilibrium but oscillate in a small cycle around the equilibrium. Although non-saturating GAN (GAN-NS) [1] was proven to be convergent under strong assumptions [13, 14], Fedus et al. [15] observed that on many real world datasets, the distance between p_g^t and p_r (measured in KL-divergence and Jensen-Shannon divergence) does not decrease as t increases. The author suggested that p_g can approach p_r in many different and unpredictable ways. These results imply that in the most common variants of GANs, p_g^t can be arbitrarily different from p_g^{t-n} for large n . If the knowledge used for separating p_g^t and p_r cannot be used for separating p_g^{t-n} and p_r , a discriminator trained on \mathcal{T}^t could forget \mathcal{T}^{t-n} , i.e. it classifies samples in \mathcal{T}^{t-n} wrongly. When this happens, we say that the discriminator exhibits catastrophic forgetting behaviors.

2.2 Catastrophic forgetting in GANs

2.2.1 Catastrophic forgetting on synthetic dataset

We begin by analyzing the problem on the 8 Gaussian dataset, a dataset generated by a mixture of 8 Gaussians placed on a circle. In Fig. 1, red datapoints are generated samples, blue datapoints are real samples. The discriminator and generator are 2 hidden layer MLP with 64 hidden neurons. ReLU activation function was used. p_z is a 2-dimensional standard normal distribution. SGD with constant learning rate of $\alpha = 3 \times 10^{-3}$ was used for both networks. The vector at a datapoint \mathbf{x} shows the negative gradient $-\partial\mathcal{L}_G/\partial\mathbf{x}$. The vector shows the direction in which \mathcal{L}_G decreases the fastest. The length of the vector corresponds to the speed of change in \mathcal{L}_G . Because the gradient field is conservative, the the difference between the loss of two datapoints \mathbf{x}_0 and \mathbf{x}_1 is:

$$\mathcal{L}_G(D(\mathbf{x}_0)) - \mathcal{L}_G(D(\mathbf{x}_1)) = \int_{\mathcal{C}} \mathbf{v} \cdot d\mathbf{s} \quad (1)$$

where $\mathbf{v} = -\partial\mathcal{L}_G/\partial\mathbf{x}$ and \mathcal{C} is a path from \mathbf{x}_0 to \mathbf{x}_1 . For the variants in Table 1, $\partial\mathcal{L}_G/\partial\mathbf{x}$ only depends on \mathbf{x} and the discriminator. Because decreasing \mathcal{L}_G in these GANs corresponds to increasing $D(\mathbf{x})$, going in the direction of $-\partial\mathcal{L}_G/\partial\mathbf{x}$ increases the score $D(\mathbf{x})$. Let $\mathbf{y}_0 = G(\mathbf{z}_0)$, $\mathbf{z}_0 \sim p_z$ be a fake datapoint. Updating \mathbf{y}_0 with SGD with a small enough learning rate will move \mathbf{y}_0 in the direction of $-\partial\mathcal{L}_G/\partial\mathbf{y}_0$ by a distance proportional to $\|-\partial\mathcal{L}_G/\partial\mathbf{y}_0\|$. If the discriminator is fixed, then SGD updates will move \mathbf{y}_0 along its integral curve, in the direction of increasing $D(\mathbf{y}_0)$.²

²In practice, gradient updates are not applied to \mathbf{y}_0 but to the generator’s parameters. Because the generator also

	\mathcal{L}_D	\mathcal{L}_G
WGANGP	$-\mathbb{E}_{\mathbf{x} \sim p_r} [D(\mathbf{x})] + \mathbb{E}_{\mathbf{z} \sim p_z} [D(G(\mathbf{z}))] + \lambda \mathbb{E}_{\mathbf{u}} [(\ \nabla D\ _{\mathbf{u}} - 1)^2]$ where $\mathbf{u} = \alpha \mathbf{x} + (1 - \alpha) \mathbf{y}$; $\mathbf{x} \sim p_x$, $\mathbf{y} \sim p_g$, $\alpha \sim \mathcal{U}(0, 1)$	$-\mathbb{E}_{\mathbf{z} \sim p_z} [D(G(\mathbf{z}))]$
GAN-NS	$\mathbb{E}_{\mathbf{x} \sim p_r} [-\log(D(\mathbf{x}))] + \mathbb{E}_{\mathbf{z} \sim p_z} [-\log(1 - D(G(\mathbf{z})))]$	$\mathbb{E}_{\mathbf{z} \sim p_z} [-\log(D(G(\mathbf{z})))]$
GAN-R1	$\mathbb{E}_{\mathbf{x} \sim p_r} [-\log(D(\mathbf{x}))] + \mathbb{E}_{\mathbf{z} \sim p_z} [-\log(1 - D(G(\mathbf{z})))] + \lambda \mathbb{E}_{\mathbf{x} \sim p_r} [\ \nabla D\ _{\mathbf{x}}^2]$	$\mathbb{E}_{\mathbf{z} \sim p_z} [-\log(D(G(\mathbf{z})))]$
GAN-0GP	$\mathbb{E}_{\mathbf{x} \sim p_r} [-\log(D(\mathbf{x}))] + \mathbb{E}_{\mathbf{z} \sim p_z} [-\log(1 - D(G(\mathbf{z})))] + \lambda \mathbb{E}_{\mathbf{u}} [\ \nabla D\ _{\mathbf{u}}^2]$ where $\mathbf{u} = \alpha \mathbf{x} + (1 - \alpha) \mathbf{y}$; $\mathbf{x} \sim p_x$, $\mathbf{y} \sim p_g$, $\alpha \sim \mathcal{U}(0, 1)$	$\mathbb{E}_{\mathbf{z} \sim p_z} [-\log(D(G(\mathbf{z})))]$

Table 1: Loss functions of GAN variants considered in this paper.

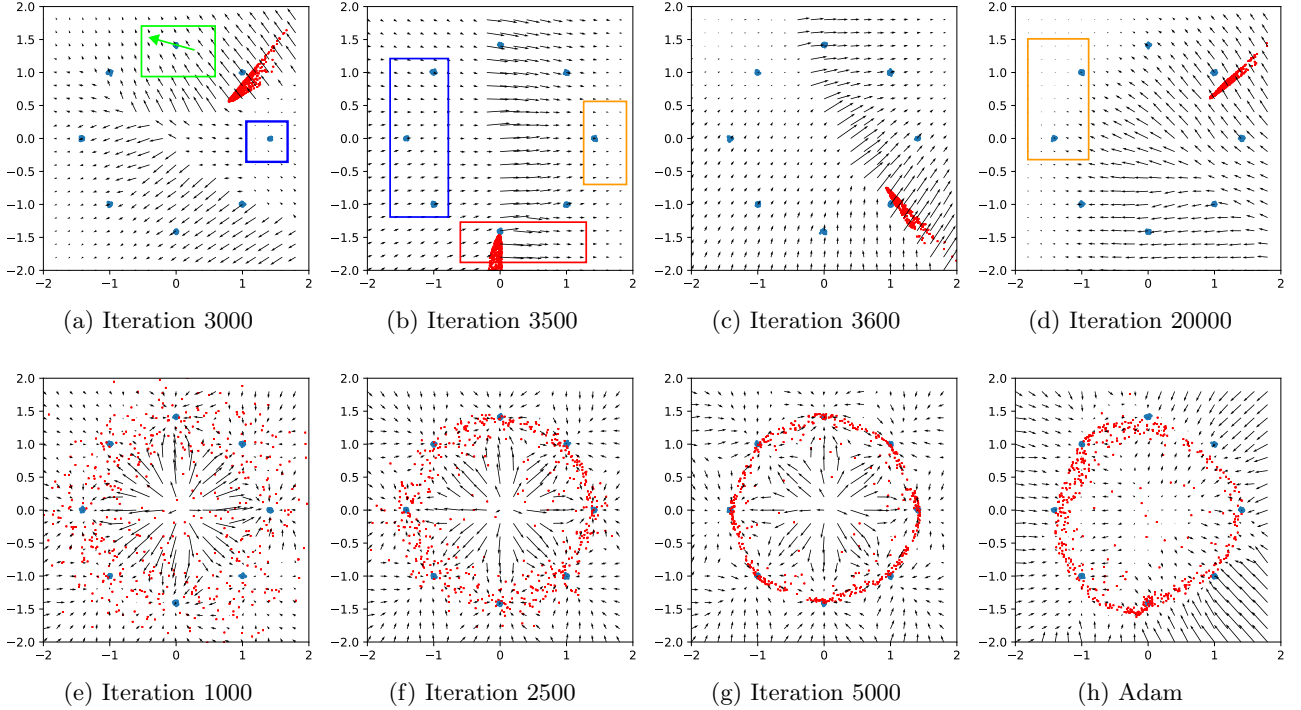


Figure 1: (a) - (d) catastrophic forgetting in GAN-NS trained on the 8 Gaussian dataset. See Fig. 9 in Appendix B for the full sequence. (e) - (g) GAN-R1 with $\lambda = 10$. GAN-0GP and WGAN-GP exhibit similar behaviors on this dataset. (h) GAN-NS trained with Adam. See Fig. 11 in Appendix B for the full sequence. Viewing on computer is recommended.

Fig. 1a - 1d show the evolution of a GAN-NS on 8 Gaussian dataset. In Fig. 1a - 1c, the discriminator assigns higher score to datapoints that are further away from the fake datapoints, regardless of the true labels of these points. In Fig. 1a, this is shown by the gradient vectors pointing away from the fake datapoints. The integral curves do not converge to any real datapoints. If D is fixed, p_g will diverge. Because gradients w.r.t. different fake datapoints have the same direction, fake datapoints move in the same direction and do not spread out over the space. The generator cannot break out of mode collapse.

minimizes \mathcal{L}_G , gradient updates to the generator move \mathbf{y}_0 in a direction that approximates $-\partial \mathcal{L}_G / \partial \mathbf{y}_0$. $-\partial \mathcal{L}_G / \partial \mathbf{y}_0$ is a good approximation of the direction that \mathbf{y}_0 will move in the next iteration.

Inside the green box, gradients at all datapoints have approximately the same direction. The loss \mathcal{L}_G decreases (the score $D(\cdot)$ increases) monotonically along the direction of the green vector \mathbf{u} , a random vector that points away from the fake datapoints.³ We have the following observation: *In a large neighborhood around a real datapoint, \mathcal{L}_G (and therefore, $D(\cdot)$) is directionally monotonic.*

³ Graphically, we see that the angles between the green vector \mathbf{u} and the gradients are all less than 90° . Thus, the dot product $\mathbf{v} \cdot d\mathbf{u}$ is positive. The line integral in Eqn. 1 is positive for $\mathbf{x}_0, \mathbf{x}_1$ in the green box that satisfy $\mathbf{x}_1 = \mathbf{x}_0 + k\mathbf{u}$, $k > 0$. \mathcal{L}_G monotonically decreases along the direction of \mathbf{u} . \mathcal{L}_G monotonically increases along the direction $-\mathbf{u}$. We say that \mathcal{L}_G is monotonic in direction \mathbf{u} .

In Fig. 1b, fake datapoints on the right of the red box have higher scores than real datapoints on the left, although in Fig. 1a, these real datapoints have higher scores than these fake datapoints. The phenomenon suggests that D overemphasizes on separating the current fake datapoints from near by real datapoints, ignoring older information. Going from Fig. 1a to 1d, we observe that the vectors' directions change as soon as fake datapoints move. Information about previous model distributions is not preserved in the discriminator. There are a number of reasons for this phenomenon:

1. *Information from previous tasks is not carried to/used for the current task.* SGD does not use information from previous model distributions, $p_g^{<t}$. At iteration t , SGD update for the discriminator is computed from samples from p_g^t and p_r only. Because information from $p_g^{<t}$ is not used for training, the discriminator forgets $p_g^{<t}$, i.e. it does not assign low score to samples from $p_g^{<t}$.
2. *The current task is significantly different from previous tasks and the knowledge of the current task cannot be used for previous tasks and vice versa.* As old knowledge is overwritten by new knowledge, optimizing the discriminator on the current task will degrade its performance on older tasks. In Fig. 1a, D^{3000} can separate p_g^{3000} from p_r by assigning lower score to samples from p_g^{3000} and higher scores to samples from p_r . However, D^{3000} does not perform well on the pair $\{p_g^{3500}, p_r\}$. The reverse is true for D^{3500} in Fig. 1b.

Methods for preventing CF is studied in Section 4.

In Fig. 1a, as the discriminator tries to separate p_g^{3000} from p_r , it assigns lower scores to fake datapoints. However, because the discriminator does not remember $p_g^{<t}$, it assigns higher score to datapoints that are further away from the fake datapoints. The discriminator continually directs the generator to move the model distribution to another region of the space, even if that region has been visited before. That makes the model distribution rotates around the circle. The discriminator and the generator fall into a learning loop and do not converge to an equilibrium. In the experiment in Fig. 1a - 1d, the loop continues for many cycles without breaking. The discriminator and generator at iteration 20000 are very similar to themselves at iteration 3000: the model distributions have the same shape and are located at the same location; the gradients around fake datapoints point in approximately the same direction.

2.2.2 Catastrophic forgetting on MNIST dataset

Fig. 2 demonstrates the problem on MNIST. The generator and discriminator are 3 hidden layer MLP with 512 hidden neurons. SGD with constant learning rate $\alpha = 3 \times 10^{-4}$ was used in training. Detailed configuration is given in Appendix C. We visualize the landscape around a real datapoint \mathbf{x} by plotting the output of the discriminator along a random line through \mathbf{x} . We choose a random unit vector $\hat{\mathbf{u}} \in \mathbb{R}^d$ and plot the value of the function

$$f(k) = D(\mathbf{x} + k\hat{\mathbf{u}}) \quad (2)$$

for $k \in [-100, 100]$. We use the same $\hat{\mathbf{u}}$ for all images in Fig. 2. We choose to visualize $D(\cdot)$ instead of \mathcal{L}_G because \mathcal{L}_G explodes if $D(\cdot) \ll 1$. The quality of the image $\mathbf{x} + k\hat{\mathbf{u}}$ decreases as $|k|$ increases (Fig. 12 in Appendix C). A good discriminator D^* should assign lower score to samples with lower quality. $D^*(\mathbf{x})$ should be higher than $D^*(\mathbf{x} + k\hat{\mathbf{u}})$, $k > 0$, i.e. \mathbf{x} is a local maximum of D^* . If \mathbf{x} is a local maximum of D^* , $f^*(k)$ must have a local maximum at $k = 0$ (the center of each subplot). The result reported below was observed in all 10 different runs of the experiment.

As shown in Fig. 2, the generated images keep changing from one shape to another, implying that the game does not converge to an equilibrium. In a large neighborhood around every real image, the discriminator's output is monotonic in the sampled direction. At iteration 100000, for every image, f is a decreasing function (Fig. 2f), while at iteration 200000, f is an increasing function (Fig. 2g). More concretely, let $\nabla_{\hat{\mathbf{u}}} D^t(\mathbf{x}_0)$ be the discriminator's directional derivative along direction $\hat{\mathbf{u}}$ at \mathbf{x}_0 at iteration t . Then Fig. 2f and 2g shows that $\nabla_{\hat{\mathbf{u}}} D^{100000}(\mathbf{x}_0)$ and $\nabla_{\hat{\mathbf{u}}} D^{200000}(\mathbf{x}_0)$ for some \mathbf{x}_0 near the real datapoint \mathbf{x} , have opposite directions. The knowledge of D^{200000} is not usable for D^{100000} . GAN-NS trained on high dimensional datasets like MNIST exhibits the same catastrophic forgetting behaviors as GAN-NS trained on toy datasets (Fig. 1a - 1d): the discriminator is directionally monotonic in the neighborhood of a real datapoint; the gradients w.r.t. datapoints in the neighborhood change their directions as fake datapoints move. Section 3 discusses the phenomenon in greater detail.

3 The output landscape

3.1 The evolution of the landscape

We apply the visualization technique in Section 2.2.2 to other variants of GAN. We reuse the network architecture and learning rate from the experiment in Fig. 2. We replace SGD with Adam with $\beta_1 = 0.5, \beta_2 = 0.99$.

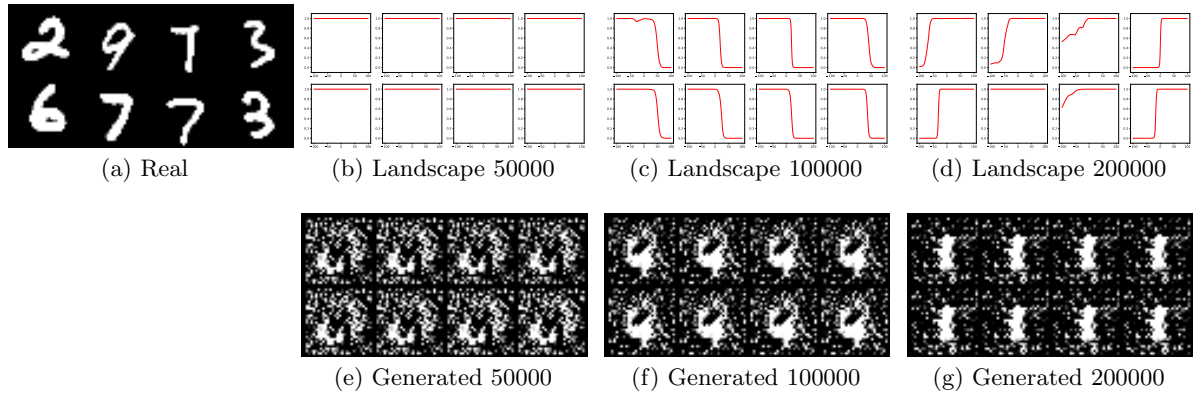


Figure 2: Catastrophic forgetting problem in GAN-NS trained with SGD. (a) real datapoints from MNIST dataset. (b) - (d) the landscape around these real datapoints at different training iterations. In each subplot, the X -axis represent k , the Y -axis represent $D(\cdot)$. (e) - (g) generated data at different iterations. The same noise inputs were used for all iterations. See Fig. 18 in Appendix C for the full figure.

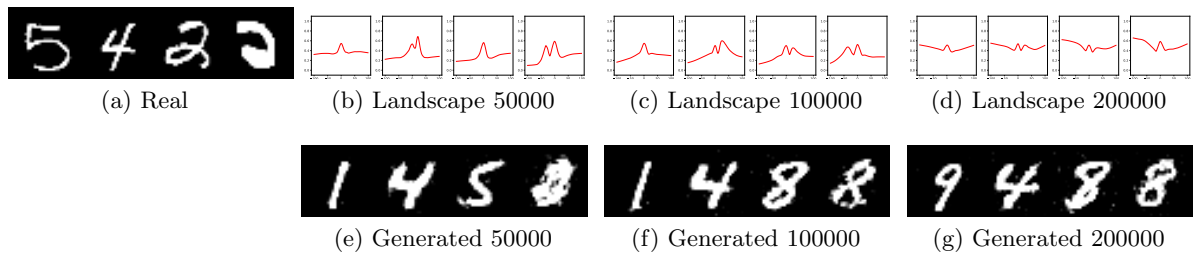


Figure 3: Output landscape and generated samples from GAN-0GP with $\lambda = 100$. See Fig. 15 in Appendix C for the full figure.

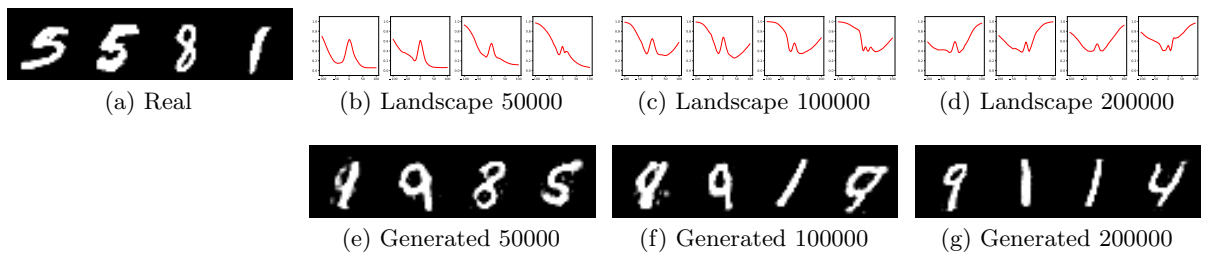


Figure 4: Output landscape and generated samples from GAN-R1, $\lambda = 100$. See Fig. 14 in Appendix C for the full figure.

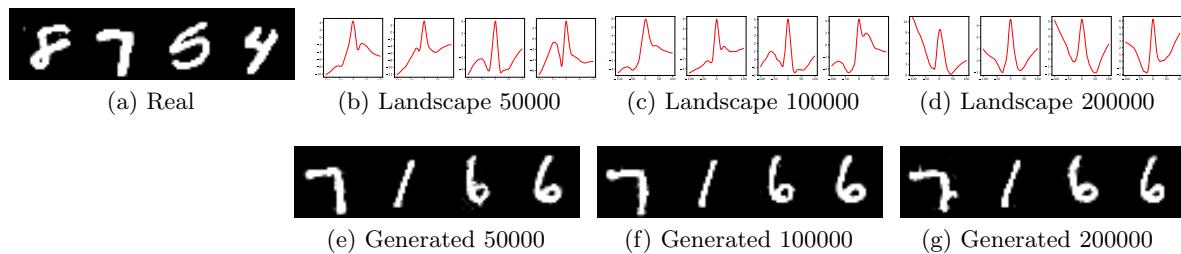


Figure 5: Output landscape and generated samples from WGAN-GP, $\lambda = 10$, 5 discriminator updates per 1 generator update. See Fig. 17 in Appendix C for the full figure.

Details about the configuration are given in Appendix C. We run each experiment 10 times with different random seeds and report results that are consistent between different runs. The evolution of the landscape and generated samples of GAN-0GP with $\lambda = 100$, GAN-R1 with $\lambda = 100$, and WGAN-GP with $\lambda = 10$ are shown in Fig. 3, 4, and 5 respectively. The result for GAN-NS trained with Adam is shown in Fig. 13 in Appendix C.

GAN-0GP, GAN-R1, and WGAN-GP have significantly better sample quality and diversity than GAN-NS. GAN-NS does not exhibit good convergence behavior: the digit in a image changes from one digit to another as the training progresses (Fig. 13).⁴ GAN-0GP, GAN-R1, and WGAN-GP exhibit better convergence behaviors: for many images, the digits stay the same during training.

We observe that throughout the training process of GAN-0GP, GAN-R1, and WGAN-GP, for every real datapoint, the function $f(k)$ always has a local maximum at $k = 0$, implying that real datapoints are local maxima of the discriminator. This can also be seen on the 8 Gaussian dataset (Fig. 1e - 1g): the gradients w.r.t. datapoints in the neighborhood of a real datapoint point toward that real datapoint. If a fake datapoint is in the basin of attraction of a real datapoint and gradient updates are applied directly on the fake datapoint, it will be attracted toward the real datapoint. Different attractors (local maxima) at different regions of the data space attract different fake datapoints toward different directions, spreading fake datapoints over the space, effectively reducing mode collapse.

Fig. 6 shows that GAN-0GP with $\lambda = 10$ suffers from mild mode collapse.⁵ The maxima in Fig. 6 are much sharper than those in Fig. 5. The discriminator overfits to the real training datapoints and forces the scores of near by datapoints to be close to 0. That creates many flat regions where the gradients of the discriminator w.r.t. datapoints in these regions are vanishingly small. It is very hard for a gradient based generator to get pass these flat regions to discover the real datapoints. The diversity of generated samples is thus reduced, making mode collapse visible.

The landscape of GAN-NS in Fig. 2 and 13 also contains many flat regions where the scores $D(\cdot)$ are very close to 1 or 0. The same problem is seen on the 8

Gaussian dataset. Datapoints in the orange boxes in Fig. 1b and 1d have scores close to 1. Datapoints in the blue boxes in Fig. 1a and 1b have scores close to 0. However, unlike Fig. 6, the real datapoints in Fig. 1a - 1d, 2, and 13 are not local maxima. The discriminator in GAN-NS underfits the data.

We make the following observation: *For a GAN to converge to a good local equilibrium, real datapoints should be wide local maxima of the discriminator.*

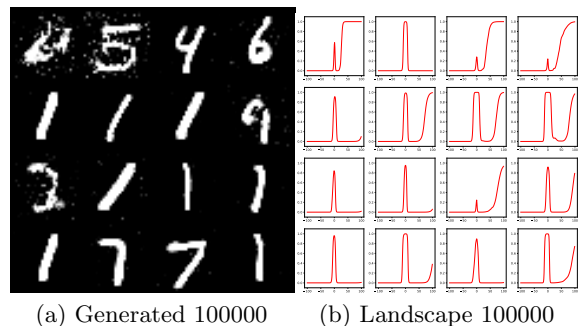


Figure 6: Mode collapse without CF in GAN-0GP, $\lambda = 10$. Full figure Fig. 16 in Appendix C.

3.2 The effect of catastrophic forgetting on the landscape

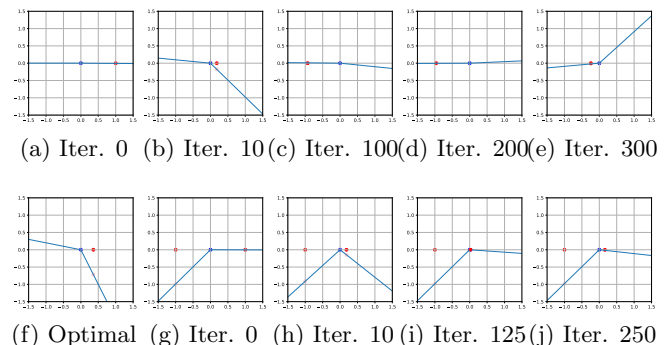


Figure 7: High capacity Dirac GAN with $n = 2$. The blue line represents the discriminator’s function. The real and fake datapoints are shown by the blue and red dots, respectively. (a) - (e): Dirac GAN trained on the current fake example only. Refer to Fig. 8 in Appendix B for the full sequence. (f): empirically optimal Dirac discriminator trained on the current fake example only. (g) - (j): Dirac GAN trained on two fake examples: old fake example on the left and current fake example on the right.

We investigate the effect of CF on Dirac GAN [8], a GAN that learns a 1 dimensional Dirac distribution located at the origin, $p_r = \delta_0$. In the original Dirac

⁴Note that this does not contradict the statement in [13] that GAN-NS converge to an equilibrium. Many of the assumptions in that paper is not satisfied in practice, e.g. the learning rate is not decayed toward 0.

⁵This is consistent with the analysis by the author of GAN-0GP. Thanh-Tung et al. claimed that larger λ leads to better generalization but may slow down the training.

GAN, the discriminator is a linear function with 1 parameter, $D(x) = \psi x$, $\psi \in [-1, 1]$ and the model distribution is a Dirac distribution located at θ , $p_g = \delta_\theta$. θ is the generator’s parameter. Initially, $\theta \neq 0$. At each iteration, the training dataset of Dirac GAN contains two training examples: a real training example $x_0 = 0$, and a fake training example $y_0 = \theta$. Gradient updates are applied directly on the fake training example.

$$-\mathcal{L}_G^{dirac} = \mathcal{L}_D^{dirac} = -D(0) + D(x) \quad (3)$$

The unique equilibrium is $\psi = \theta = 0$. Mescheder et al. showed that the players in Dirac GAN do not converge to an equilibrium (see Fig. 1 in [8]). To make the game converge to the above equilibrium, the authors proposed R1 gradient penalty which pushes the gradient w.r.t. the real datapoint to $\mathbf{0}$ (Table 1).

Different from the landscape of GAN-R1 in Fig. 4, the landscape of Dirac GAN-R1 is always a monotonic function without any local maxima. This is because the discriminator in Dirac GAN is a linear function with a single parameter. We consider a more generic discriminator which is a 1 hidden layer neural network: $\hat{D}(x) = \Psi_1^\top \sigma(\Psi_0 x)$ where $\Psi_0, \Psi_1 \in [-1, 1]^{n \times 1}$, and σ is a monotonically increasing activation function such as Leaky ReLU (Fig. 7). At equilibrium, $\theta = 0$ and $\hat{D}(x)$ is any function with a global maximum at $x = 0$. Although \hat{D} can have global maxima (see Fig. 7h), optimizing \hat{D} on the current pair of distributions tends to make \hat{D} a monotonic function (Fig. 7f).

Proposition 1. *The optimal Dirac discriminator $\hat{D}^*(x)$ that minimizes \mathcal{L}_D^{dirac} in Eqn. 3 is a monotonic function.*

Proof. See Appendix A. \square

Optimizing the performance of \hat{D} pushes it toward \hat{D}^* , making \hat{D} monotonic (Fig. 7a - 7e). This also explains the directional monotonicity of the discriminators in 1a - 1d, and 2.

Although the discriminator in Fig. 7f minimizes the score of the current fake datapoint, it assigns high scores to (old) fake datapoints on the left of the real datapoint. Because the discriminator cannot access old fake datapoints, it forgets these datapoints. If the discriminator is fixed, then minimizing \mathcal{L}_G^{dirac} corresponds to moving θ to $-\infty$. *Dirac GAN with a monotonic discriminator does not converge.* When the generator and discriminator are trained with alternating SGD, the two players oscillate around the equilibrium (Fig. 7a - 7e).

The problem can be alleviated if we store one old fake datapoint and add it to the training dataset. Fig. 7g - 7j shows that when old fake example is added, Dirac

GAN has better convergence (the small fluctuation is due to the large constant learning rate of 0.1). The discriminator at iteration 10 has a global maximum at the origin. If the discriminator is fixed, then θ will converge to 0. The experiment suggests that information about previous model distributions helps GANs converge. However, because the number of samples needed to capture the statistics of a distribution grows exponentially with its dimensionality, storing old fake datapoints is not efficient for high dimensional data. In the next section, we study more efficient methods for preserving information about old distributions.

4 Preventing catastrophic forgetting

Based on the reasons identified in Section 2.2, we propose the following ways to address CF problem:

1. *Preserve and use information from previous tasks in the current task.*
2. *Introduce prior knowledge to the game in a way such that old knowledge is useful for the new task and is not erased by the new task.*

4.1 Preserving and using old information

Optimizers with momentum. The update rule of SGD with momentum

$$\begin{aligned} \mathbf{g}^t &= \gamma \mathbf{g}^{t-1} + \eta \nabla_{\theta}^t \\ \theta^{t+1} &= \theta^t - \mathbf{g}^t \end{aligned}$$

The momentum term $\gamma \mathbf{g}^{t-1}$ is a simple form of memory that carries gradient information from previous training iterations to the current iteration. When the discriminator/generator is updated with \mathbf{g}^t , the performance of the network on previous tasks is also improved. The effectiveness of momentum in preventing forgetting is demonstrated in Fig. 1h and Fig. 11 in Appendix B. Fig. 11 shows that when the model distribution move from one mode to another, the gradient field remains stable, implying that old information is preserved in the discriminator.

Continual learning methods such as Elastic Weight Consolidation (EWC) [2] and Synaptic Intelligence (SI) [16] prevent important knowledge of previous tasks from being overwritten by the new task. At the end of a task \mathcal{T}^t , EWC computes the importance ω_i of each parameter θ_i to the task. A regularization term is added to the loss function of task \mathcal{T}^{t+1} :

$$\mathcal{L}_{EWC}^{t+1} = \mathcal{L}^{t+1} + \lambda \sum_i \omega_i (\theta_i - \theta_i^t)^2$$

where θ_i^t is the value of θ_i at the end of task \mathcal{T}^t . The regularizer prevents important weights from deviating

too far from the values that are optimal for the previous task while allowing less important weights to change more freely. EWC can help the discriminator preserves important information about old distributions. Liang et al. independently proposed a similar way of adapting continual learning methods to GANs.⁶ Experiments in the paper showed that continual learning methods improve the quality of GANs.

4.2 Introducing prior knowledge to the game

In Dirac GAN, if the discriminator has a local maximum at the real datapoint then it can always classify the real and the fake datapoint correctly, regardless of location of the fake datapoint. Because separating different fake distributions from the target distribution requires the same knowledge, that knowledge will not be erased from the discriminator. We want to introduce to the game the knowledge that real datapoints should be local maxima. R1 and 0GP are two ways to implement that.

R1 regularizer (the third row in Table 1) forces the gradients w.r.t. a real datapoint to be $\mathbf{0}$, making it a local extremum of the discriminator. As the discriminator maximizes the score of real datapoints, real datapoints become local maxima of the discriminator. Fig. 1e - 1g shows that real datapoints are always local maxima and the gradient pattern of the discriminator stay unchanged as p_g moves toward p_r . Fig. 4 demonstrates the same effect of R1 on MNIST. Note that noisy images that are far away from the real images (e.g. $\mathbf{x} + k\hat{\mathbf{u}}$ for $k < -50$) have higher scores than real images. This is because no regularizer is applied to these noisy images.

0GP regularizer (the forth row in Table 1) pushes gradients w.r.t. datapoints on the line connecting a real datapoint \mathbf{x} and a fake datapoint \mathbf{y} toward $\mathbf{0}$. 0GP forces the score to increase gradually as we move from \mathbf{y} to \mathbf{x} . During training, \mathbf{x} is paired with different \mathbf{y}_i . Thus, the score $D(\mathbf{x})$ is greater than the scores of fake datapoints in a wider neighborhood. That fixes the problem of R1 and creates wider local maxima (Fig. 3). Although generalization is beyond the scope of this paper, we believe that the sharpness of the discriminator’s landscape is related to its generalization capability. Prior works on generalization of neural networks [18] showed flat (wide) minima of the loss surface generalize better than sharp minima. Creating discriminator with wide local maxima is a good way to improve generalization of GANs.

WGAN-GP (the first row in Table 1) uses 1-centered

⁶Liang et al. agreed that we are the first to consider the catastrophic forgetting problem in GANs. The paper has not been published at any conference or journal.

gradient penalty (1GP) which pushes gradients w.r.t. datapoints on the line connecting a real datapoint \mathbf{x} and a fake datapoint \mathbf{y} toward $\mathbf{1}$, forcing the score to increase gradually from \mathbf{y} to \mathbf{x} . Fig. 5 shows that real datapoints are local maxima of the discriminator (critic). Wu et al. showed that WGAN-0GP performs slightly better than WGAN-1GP. Our hypothesis is that 0GP creates wider maxima than 1GP as it make the score on line from \mathbf{y} to \mathbf{x} change more slowly.

5 Related works

Convergence. Prior works on the convergence of GANs usually consider the convergence in parameter space [13, 14, 20, 8]. However, convergence in parameter space tells little about the quality of the equilibrium that a GAN converge to. Thanh-Tung et al. demonstrated that TTUR [14] can make GAN converge to collapse equilibrium. Consensus Optimization [20] can introduce spurious local equilibrium to the game.

We directly study the behaviors of GANs in the data space. By analyzing the discriminator’s output landscape, we find that when a GAN converge, real datapoints are local maxima of the discriminator. We discover the relationship between the sharpness of local maxima and mode collapse.

Catastrophic forgetting. Liang et al. [17] independently came up with a similar intuition that GAN training is a continual learning problem. The paper, however, did not study the causes and effects of the problem and focused on applying continual learning algorithms to address catastrophic forgetting in GANs. We focus on explaining the causes and effect of the problem and its relationship to mode collapse and non-convergence.

6 Conclusion

Catastrophic forgetting is a important problem in GANs. It is directly related to mode collapse and non-convergence. Addressing catastrophic forgetting leads to better convergence and less mode collapse. Methods such as zero centered gradient penalties, optimizers with momentum, and continual learning methods are effective at preventing catastrophic forgetting in GANs. 0GP helps GANs to converge to good local equilibria where real datapoints are wide local maxima of the discriminator. The gradient penalty is a promising method for improving generalization of GANs.

References

- [1] Ian Goodfellow, Jean Pouget-Abadie, Mehdi Mirza, Bing Xu, David Warde-Farley, Sherjil

- Ozair, Aaron Courville, and Yoshua Bengio. Generative adversarial nets. In Z. Ghahramani, M. Welling, C. Cortes, N. D. Lawrence, and K. Q. Weinberger, editors, *Advances in Neural Information Processing Systems 27*, pages 2672–2680. Curran Associates, Inc., 2014.
- [2] James Kirkpatrick, Razvan Pascanu, Neil Rabinowitz, Joel Veness, Guillaume Desjardins, Andrei A. Rusu, Kieran Milan, John Quan, Tiago Ramalho, Agnieszka Grabska-Barwinska, Demis Hassabis, Claudia Clopath, Dharshan Kumaran, and Raia Hadsell. Overcoming catastrophic forgetting in neural networks. *Proceedings of the National Academy of Sciences*, 114(13):3521–3526, 2017. ISSN 0027-8424. doi: 10.1073/pnas.1611835114.
- [3] Robert M. French. Catastrophic forgetting in connectionist networks. *Trends in Cognitive Sciences*, 3(4):128 – 135, 1999. ISSN 1364-6613. doi: [https://doi.org/10.1016/S1364-6613\(99\)01294-2](https://doi.org/10.1016/S1364-6613(99)01294-2).
- [4] Michael McCloskey and Neal J. Cohen. Catastrophic interference in connectionist networks: The sequential learning problem. volume 24 of *Psychology of Learning and Motivation*, pages 109 – 165. Academic Press, 1989. doi: [https://doi.org/10.1016/S0079-7421\(08\)60536-8](https://doi.org/10.1016/S0079-7421(08)60536-8).
- [5] Roger Ratcliff. Connectionist models of recognition memory: constraints imposed by learning and forgetting functions. *Psychological review*, 97(2): 285, 1990.
- [6] Martin Arjovsky, Soumith Chintala, and Léon Bottou. Wasserstein generative adversarial networks. In Doina Precup and Yee Whye Teh, editors, *Proceedings of the 34th International Conference on Machine Learning*, volume 70 of *Proceedings of Machine Learning Research*, pages 214–223, International Convention Centre, Sydney, Australia, 06–11 Aug 2017. PMLR.
- [7] Ishaan Gulrajani, Faruk Ahmed, Martin Arjovsky, Vincent Dumoulin, and Aaron C Courville. Improved training of wasserstein gans. In I. Guyon, U. V. Luxburg, S. Bengio, H. Wallach, R. Fergus, S. Vishwanathan, and R. Garnett, editors, *Advances in Neural Information Processing Systems 30*, pages 5767–5777. Curran Associates, Inc., 2017.
- [8] Lars Mescheder, Andreas Geiger, and Sebastian Nowozin. Which training methods for GANs do actually converge? In Jennifer Dy and Andreas Krause, editors, *Proceedings of the 35th International Conference on Machine Learning*, volume 80 of *Proceedings of Machine Learning Research*, pages 3478–3487, Stockholmssan, Stockholm Sweden, 10–15 Jul 2018. PMLR.
- [9] Hoang Thanh-Tung, Truyen Tran, and Svetha Venkatesh. Improving generalization and stability of generative adversarial networks. In *International Conference on Learning Representations*, 2019.
- [10] Sanjeev Arora, Rong Ge, Yingyu Liang, Tengyu Ma, and Yi Zhang. Generalization and equilibrium in generative adversarial nets (GANs). In Doina Precup and Yee Whye Teh, editors, *Proceedings of the 34th International Conference on Machine Learning*, volume 70 of *Proceedings of Machine Learning Research*, pages 224–232, International Convention Centre, Sydney, Australia, 06–11 Aug 2017. PMLR.
- [11] Sanjeev Arora, Andrej Risteski, and Yi Zhang. Do GANs learn the distribution? some theory and empirics. In *International Conference on Learning Representations*, 2018.
- [12] Pengchuan Zhang, Qiang Liu, Dengyong Zhou, Tao Xu, and Xiaodong He. On the discrimination-generalization tradeoff in GANs. In *International Conference on Learning Representations*, 2018.
- [13] Vaishnavh Nagarajan and J. Zico Kolter. Gradient descent gan optimization is locally stable. In I. Guyon, U. V. Luxburg, S. Bengio, H. Wallach, R. Fergus, S. Vishwanathan, and R. Garnett, editors, *Advances in Neural Information Processing Systems 30*, pages 5585–5595. Curran Associates, Inc., 2017.
- [14] Martin Heusel, Hubert Ramsauer, Thomas Unterthiner, Bernhard Nessler, and Sepp Hochreiter. Gans trained by a two time-scale update rule converge to a local nash equilibrium. In I. Guyon, U. V. Luxburg, S. Bengio, H. Wallach, R. Fergus, S. Vishwanathan, and R. Garnett, editors, *Advances in Neural Information Processing Systems 30*, pages 6626–6637. Curran Associates, Inc., 2017.
- [15] William Fedus, Mihaela Rosca, Balaji Lakshminarayanan, Andrew M. Dai, Shakir Mohamed, and Ian Goodfellow. Many paths to equilibrium: GANs do not need to decrease a divergence at every step. In *International Conference on Learning Representations*, 2018.
- [16] Friedemann Zenke, Ben Poole, and Surya Ganguli. Continual learning through synaptic intelligence. In Doina Precup and Yee Whye Teh, editors, *Proceedings of the 34th International Conference on Machine Learning*, volume 70 of *Proceedings of Machine Learning Research*, pages 3987–3995, International Convention Centre, Sydney, Australia, 06–11 Aug 2017. PMLR.
- [17] Kevin J Liang, Chunyuan Li, Guoyin Wang, and

Lawrence Carin. Generative Adversarial Network Training is a Continual Learning Problem. *arXiv e-prints*, art. arXiv:1811.11083, Nov 2018.

- [18] Sepp Hochreiter and Jürgen Schmidhuber. Flat minima. *Neural Computation*, 9(1):1–42, 1997.
- [19] Jiqing Wu, Zhiwu Huang, Janine Thoma, Dinesh Acharya, and Luc Van Gool. Wasserstein divergence for gans. In *Proceedings of the European Conference on Computer Vision (ECCV)*, pages 653–668, 2018.
- [20] Lars Mescheder, Sebastian Nowozin, and Andreas Geiger. The numerics of gans. In I. Guyon, U. V. Luxburg, S. Bengio, H. Wallach, R. Fergus, S. Vishwanathan, and R. Garnett, editors, *Advances in Neural Information Processing Systems 30*, pages 1825–1835. Curran Associates, Inc., 2017.

A Proof for Proposition 1

Proof. Let $\hat{D}(x) = \Psi_1^\top \sigma(\Psi_0 x)$ where $\Psi_0, \Psi_1 \in [-1, 1]^{n \times 1}$ be the discriminator and σ be a non-decreasing activation function such as ReLU, Leaky ReLU, Sigmoid, or Tanh. Let $x_0 = 0$ be the real datapoint, $y_0 = \theta \neq 0$ be the fake datapoint. The empirically optimal discriminator D^* must maximize the difference $D^*(x_0) - D^*(y_0)$.

$$\begin{aligned} \hat{D}(x_0) &= \Psi_1^\top \sigma(\Psi_0 \times 0) \\ &= \Psi_1^\top \sigma(\mathbf{0}) \\ &= \sum_{i=1}^n \Psi_{1,i} \sigma(0) \\ \hat{D}(y_0) &= \Psi_1^\top \sigma(\Psi_0 \times y_0) \\ &= \sum_{i=1}^n \Psi_{1,i} \sigma(\Psi_{0,i} y_0) \\ \hat{D}(x_0) - \hat{D}(y_0) &= \sum_{i=1}^n \Psi_{1,i} \times (\sigma(0) - \sigma(\Psi_{0,i} y_0)) \end{aligned}$$

Because

$$\Psi_{0,i} y_0 \leq |y_0|$$

and σ is non-decreasing

$$\sigma(0) - \sigma(-|y_0|) \geq \sigma(0) - \sigma(\Psi_{0,i} y_0) \geq \sigma(0) - \sigma(|y_0|)$$

If σ is ReLU or Leaky ReLU or Tanh, then $\sigma(0) = 0$, $|\sigma(|y_0|)| \geq |\sigma(-|y_0|)|$, thus

$$|\sigma(0) - \sigma(|y_0|)| > |\sigma(0) - \sigma(-|y_0|)|$$

If σ is Sigmoid, then $\sigma(0) = 0.5$ and $|\sigma(0) - \sigma(|y_0|)| = |\sigma(0) - \sigma(-|y_0|)|$. For both cases, we have

$$|\sigma(0) - \sigma(\Psi_{0,i} y_0)| \leq |\sigma(0) - \sigma(|y_0|)| \quad (4)$$

Thus

$$\Psi_{1,i} (\sigma(0) - \sigma(\Psi_{0,i} y_0)) \leq 1 \times |\sigma(0) - \sigma(|y_0|)| \quad (5)$$

The equality for both Eqn. 1 and 2 is achieved for all cases when $\Psi_{1,i} = -1$ and $\sigma(\Psi_{0,i} y_0) = \sigma(|y_0|) \Rightarrow \Psi_{0,i} y_0 = |y_0| \Rightarrow \Psi_{0,i} = \text{sign}(y_0)$. The optimal discriminator’s parameters are $\Psi_0^* = \text{sign}(y_0) \times \mathbf{1}$, $\Psi_1^* = -\mathbf{1}$.

$$D(x) = -\mathbf{1}^\top \sigma(x \times \text{sign}(y_0) \times \mathbf{1})$$

Without loss of generality, assume $\text{sign}(y_0) = 1$.

$$D(x) = -\mathbf{1}^\top \sigma(x \times \mathbf{1}) = -n\sigma(x)$$

Because σ is monotonic, $D(x)$ is monotonic. \square

If σ is the Leaky ReLU activation function, the optimal discriminator is

$$\hat{D}^*(x) = \begin{cases} -n|x| & \text{if } x \times y_0 > 0 \\ \alpha \times n|x| & \text{if } x \times y_0 < 0 \end{cases}$$

where $\alpha \ll 1$ is the negative slope of the Leaky ReLU activation function. \hat{D}^* is a monotonic function.

The empirically optimal discriminator with $n = 2$, $y_0 > 0$ and Leaky ReLU activation function is shown in Fig. 7f.

B Experiments on synthetic datasets

C Landscapes of different GANs

This section includes figures for different GANs. The general configuration for all experiments are shown in Table 2. Hyper parameters specific to each experiment is shown in the caption of the corresponding figure.

In each figure, the ‘Real’ subfloat shows real samples from MNIST dataset. Each cell in a ‘Landscape’ subfloat shows a slice of the landscape - the value of $f(k)$, $k \in [-100, 100]$, for the corresponding real sample at the specified iteration. Each ‘Generated’ subfloat shows the generated samples at that iteration.

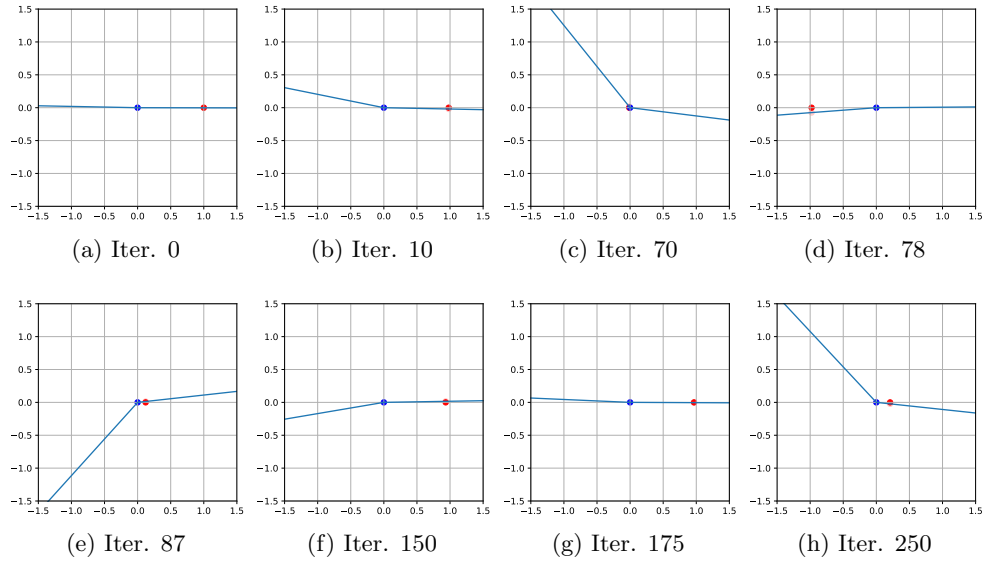


Figure 8: Catastrophic forgetting in high capacity Dirac GAN. The discriminator is a 1 hidden layer neural network with Leaky ReLU activation function and 2 hidden neurons. Although the discriminator has enough capacity to become a non-monotonic function, catastrophic forgetting makes it a monotonic function. High capacity Dirac GAN still oscillates around the equilibrium.

Architecture	3 hidden layer MLP
Hidden layer activation	ReLU
Output layer activation	Sigmoid for GAN-NS, Linear for WGAN
Number of hidden neurons	512
Latent dimensionality	50
Optimizer	ADAM with $\beta - 1 = 0.5, \beta - 2 = 0.99$
Learning rate	3×10^{-4}
Batch size	64

Table 2: Experiments configuration

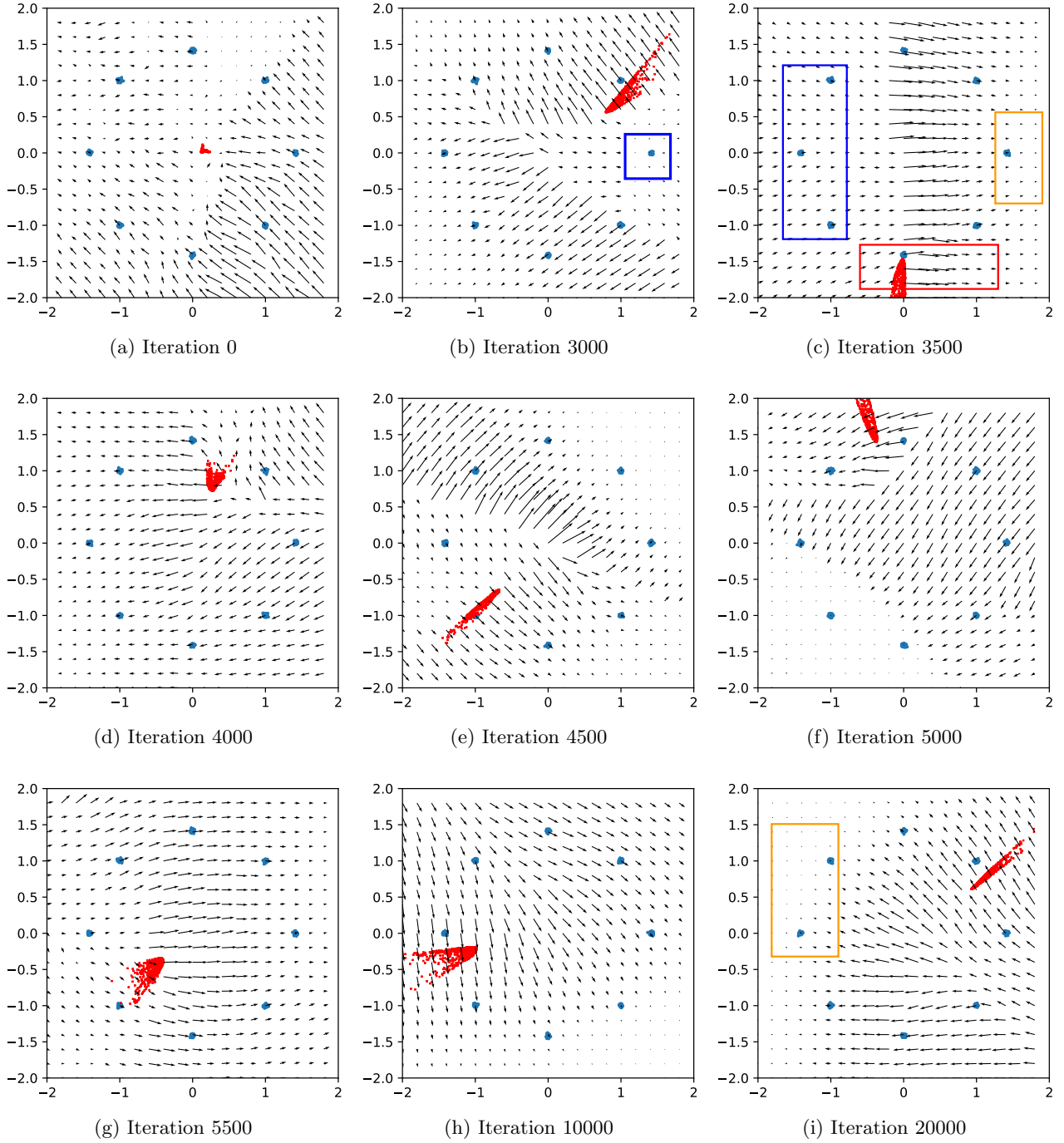


Figure 9: Catastrophic forgetting on the 8 Gaussian dataset.

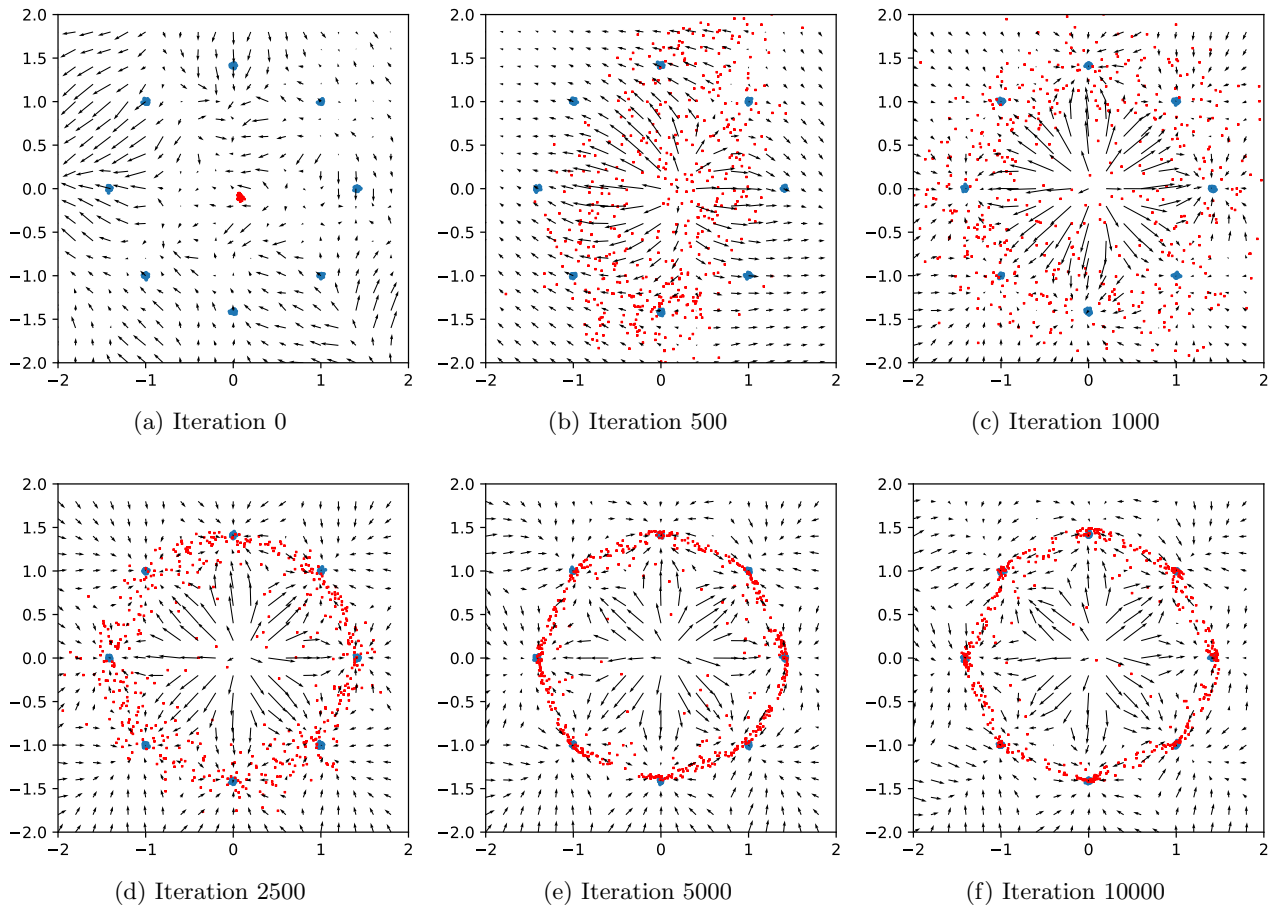


Figure 10: GAN-R1 with $\lambda = 10$ on 8 Gaussian dataset.

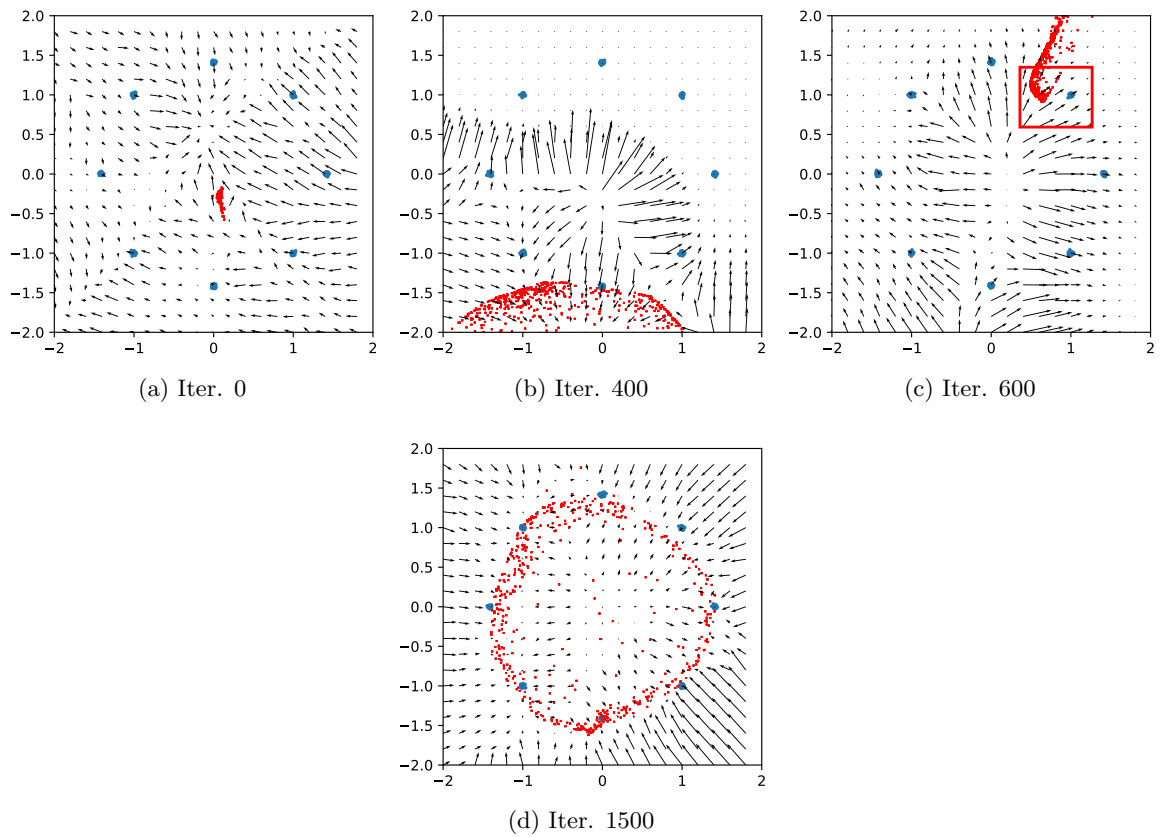


Figure 11: Evolution sequence of GAN-NS with Adam on the 8 Gaussian dataset. The gradient pattern is much more stable than that of GAN-NS with SGD. Note that the gradients in the red box still point toward the real datapoint despite the fact that the fake datapoints are close.

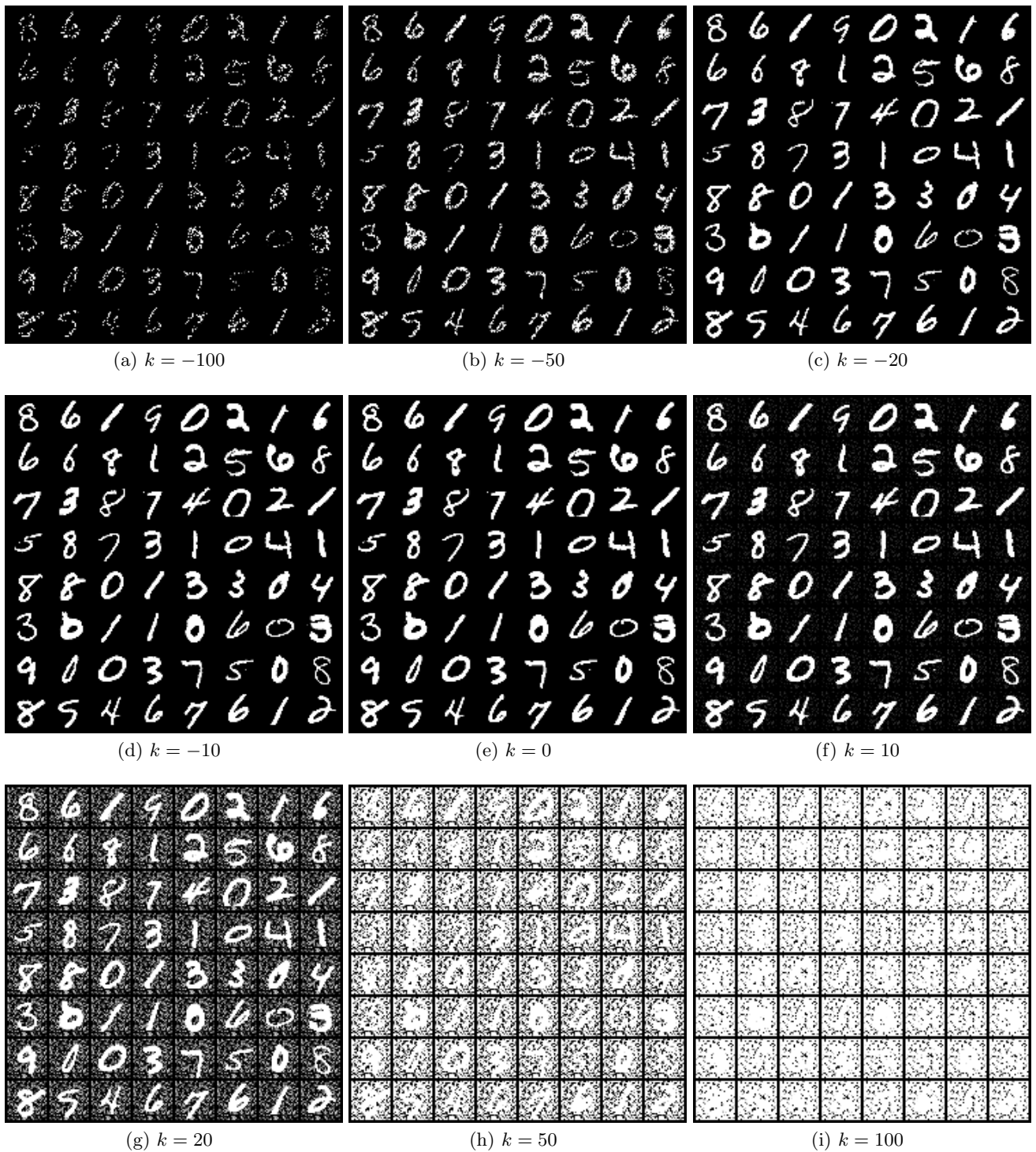
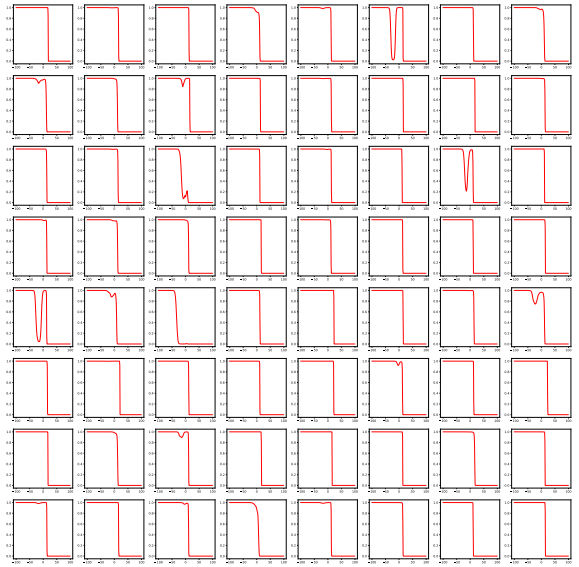


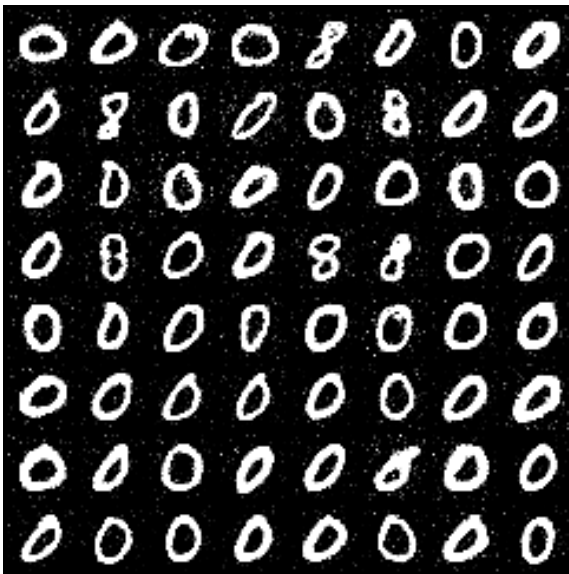
Figure 12: Real examples with different levels of noise.



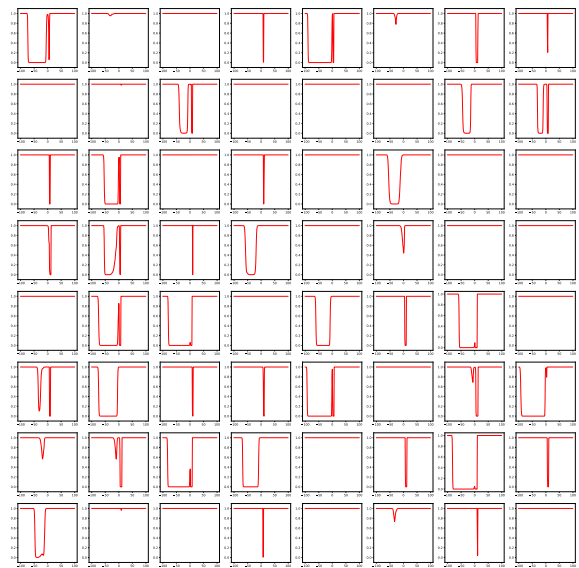
(a) Real



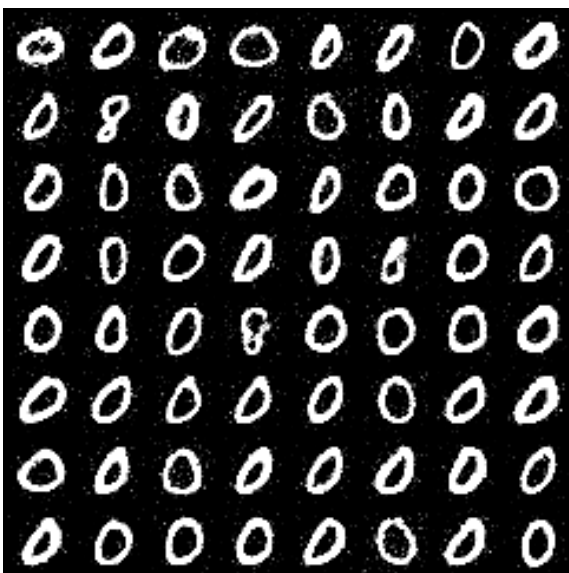
(b) Landscape 5000



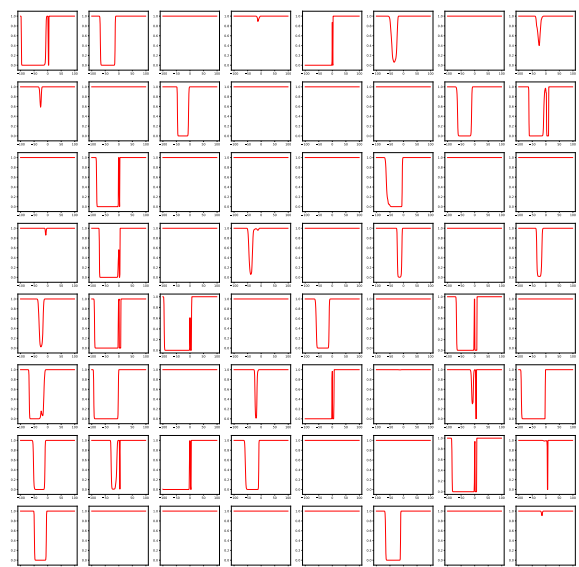
(c) Generated 50000



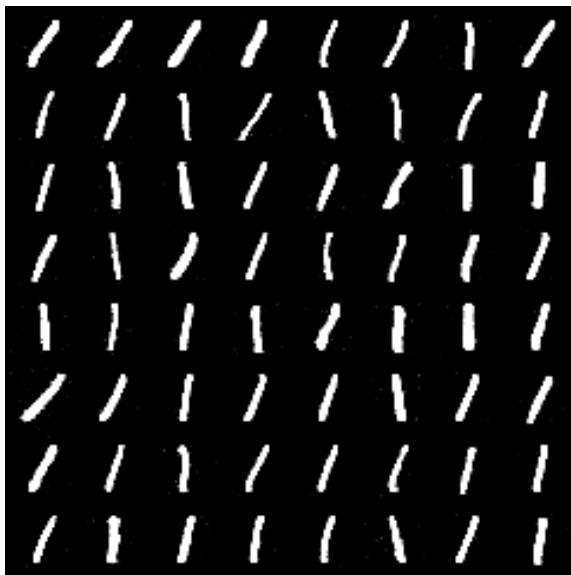
(d) Landscape 50000



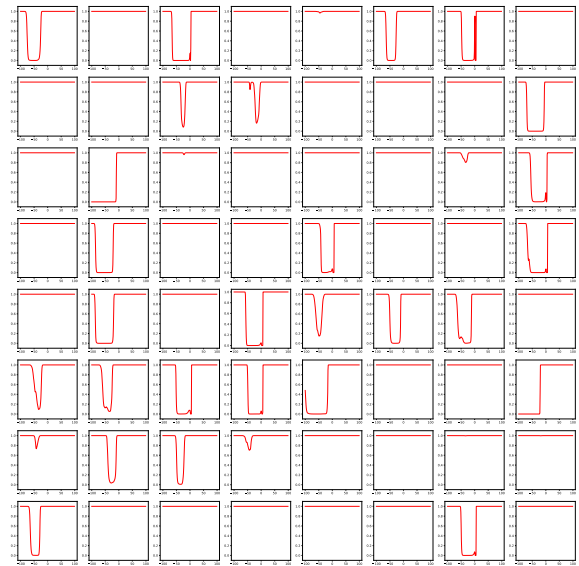
(e) Generated 100000



(f) Landscape 100000



(g) Generated 200000

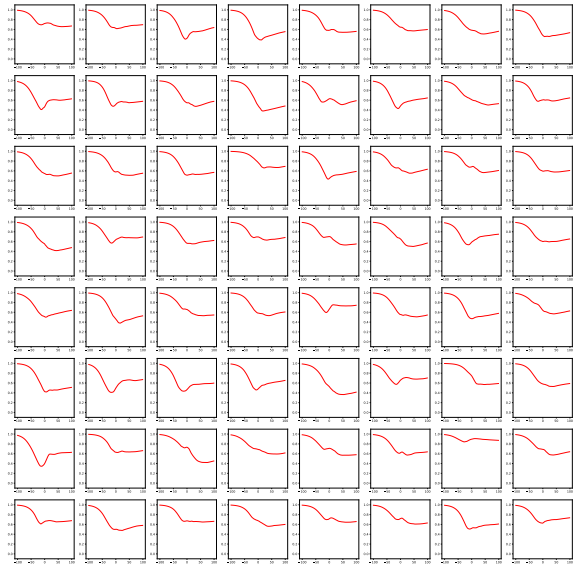


(h) Landscape 200000

Figure 13: GAN-NS



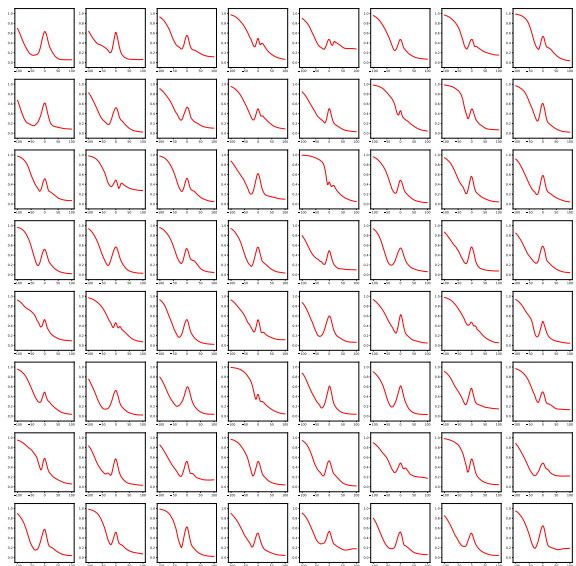
(a) Real



(b) Landscape 5000



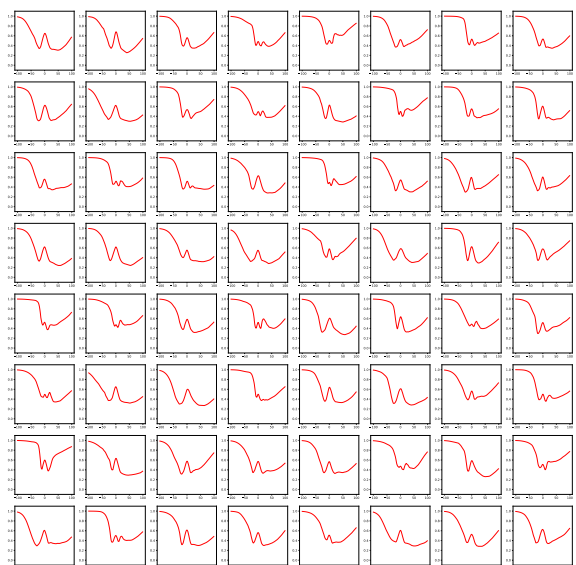
(c) Generated 50000



(d) Landscape 50000



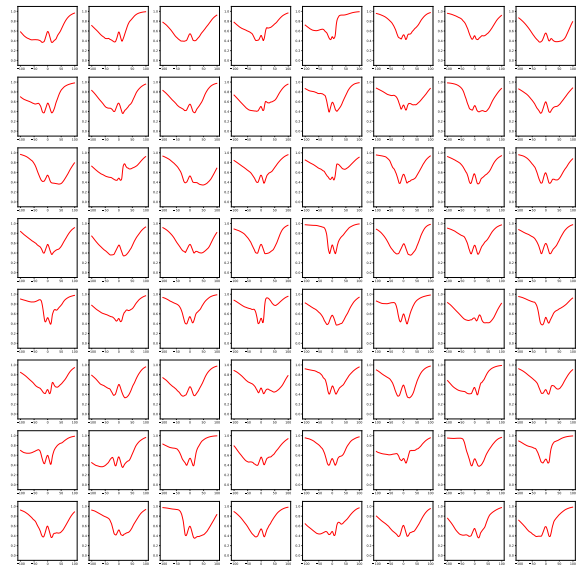
(e) Generated 100000



(f) Landscape 100000



(g) Generated 200000

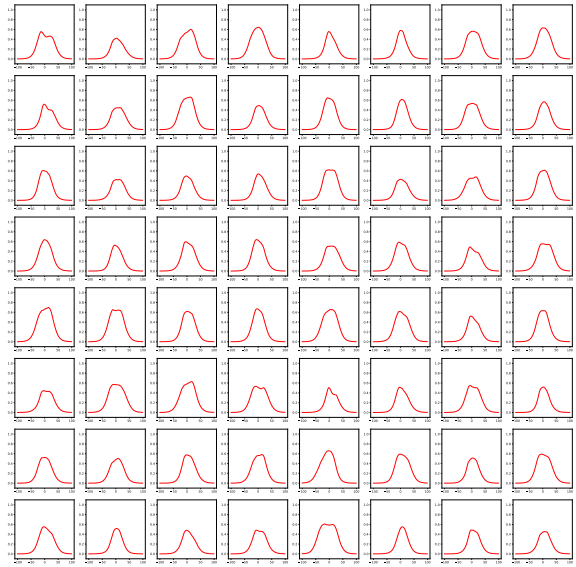


(h) Landscape 200000

Figure 14: GAN-R1, $\lambda = 100$



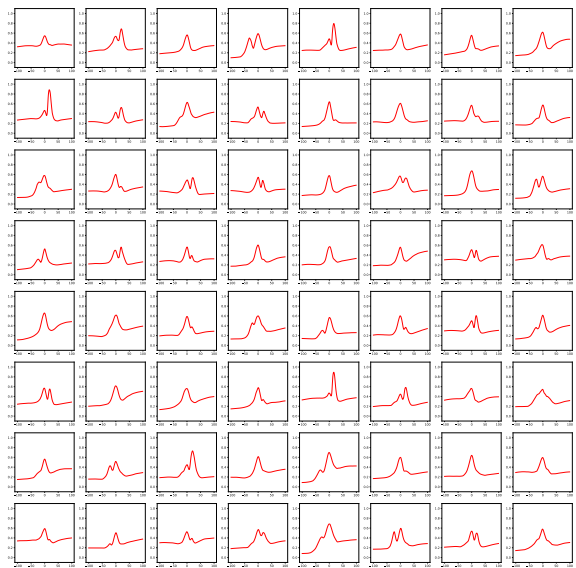
(a) Real



(b) Landscape 5000



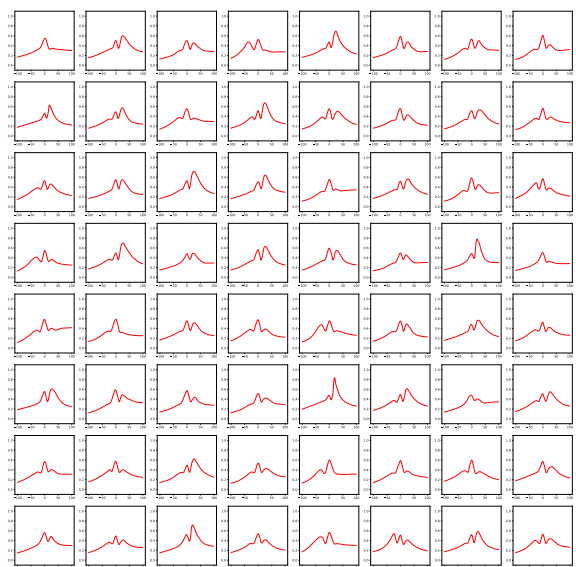
(c) Generated 50000



(d) Landscape 50000



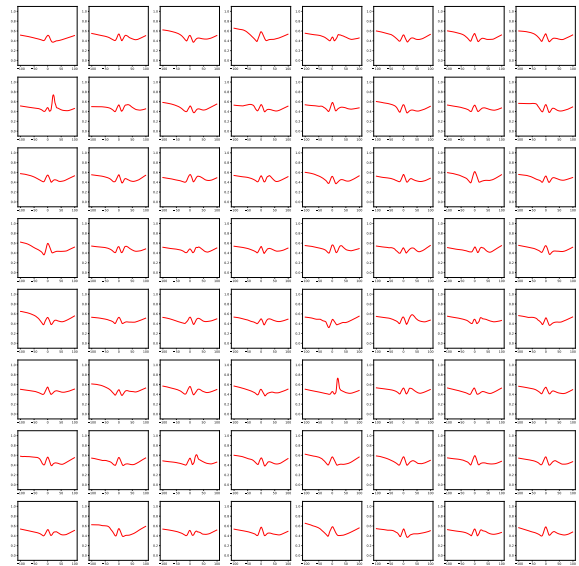
(e) Generated 100000



(f) Landscape 100000

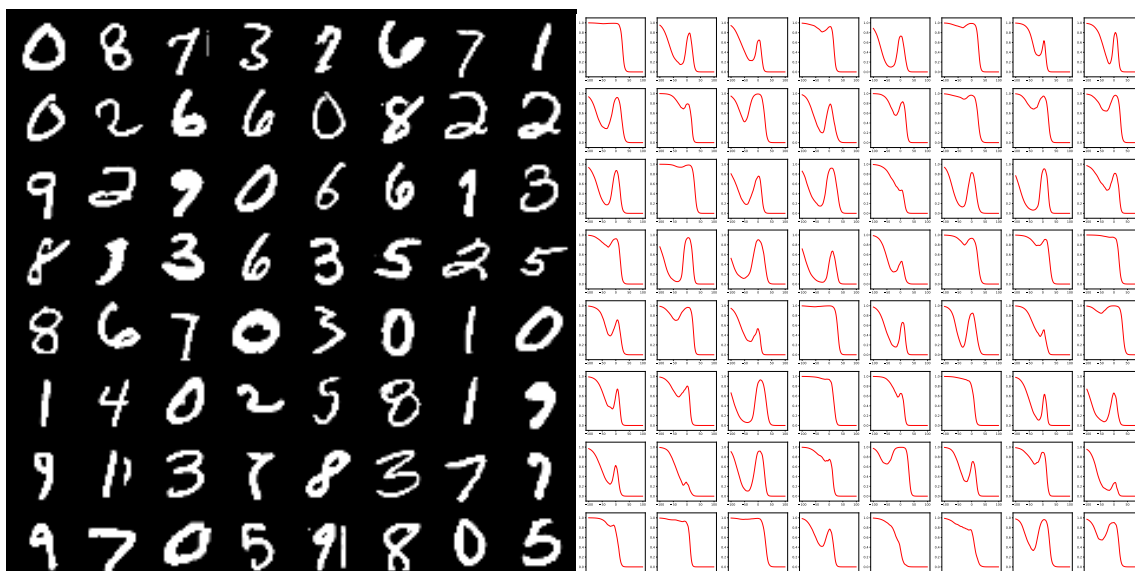


(g) Generated 200000



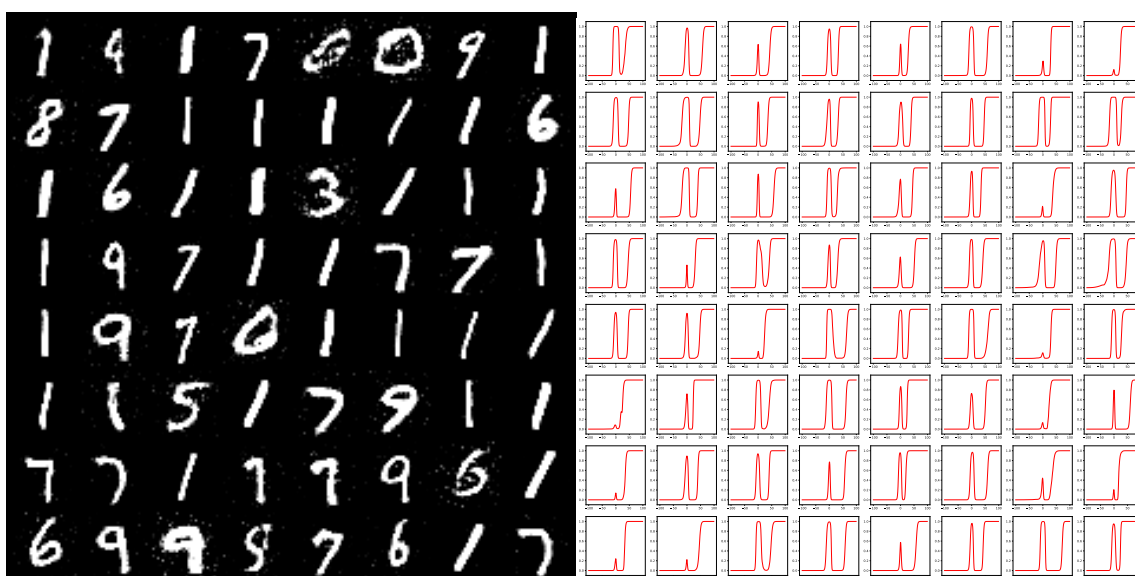
(h) Landscape 200000

Figure 15: GAN-0GP, $\lambda = 100$.



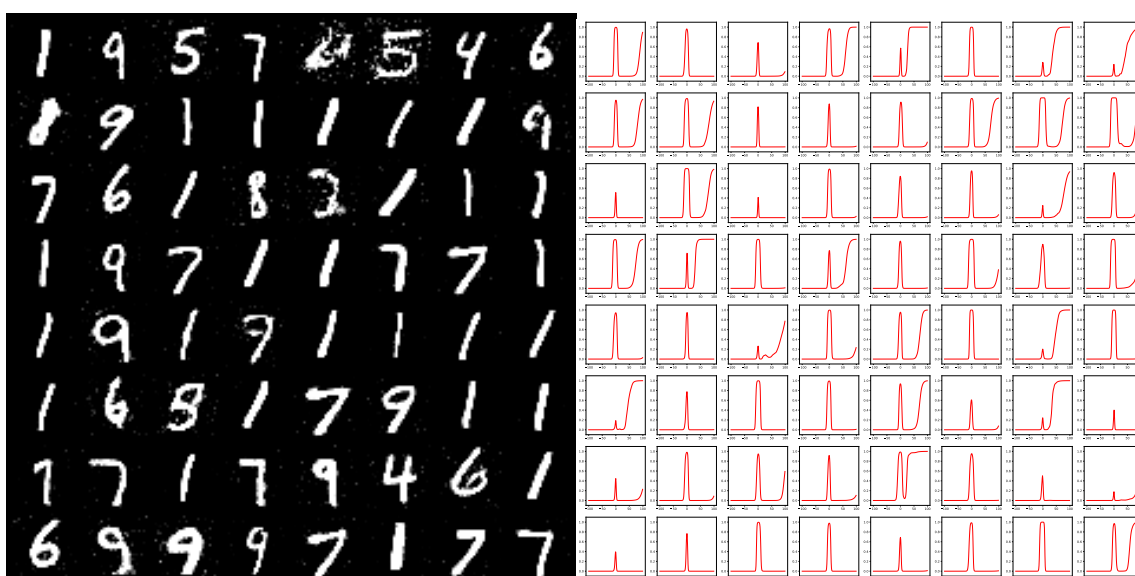
(a) Real

(b) Landscape 5000



(c) Generated 50000

(d) Landscape 50000



(e) Generated 100000

(f) Landscape 100000

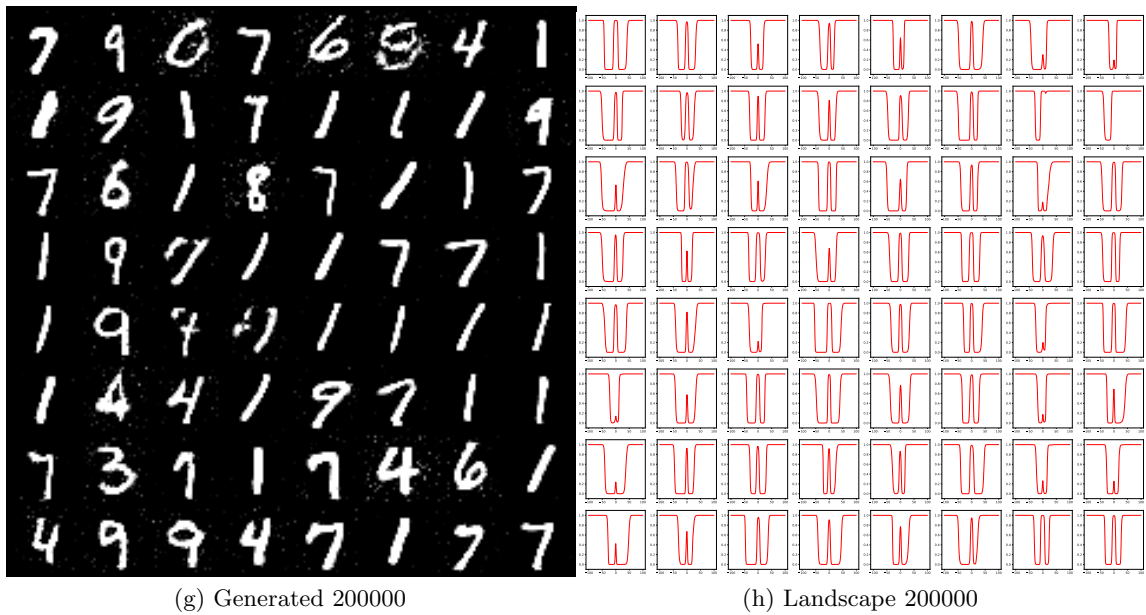
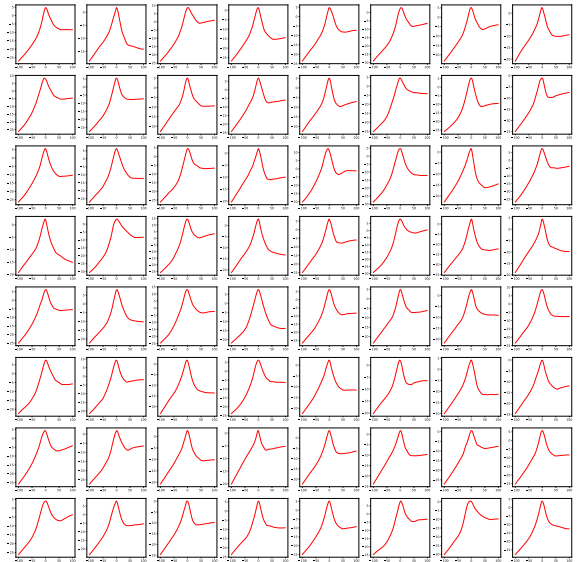


Figure 16: GAN-0GP with $\lambda = 10$.



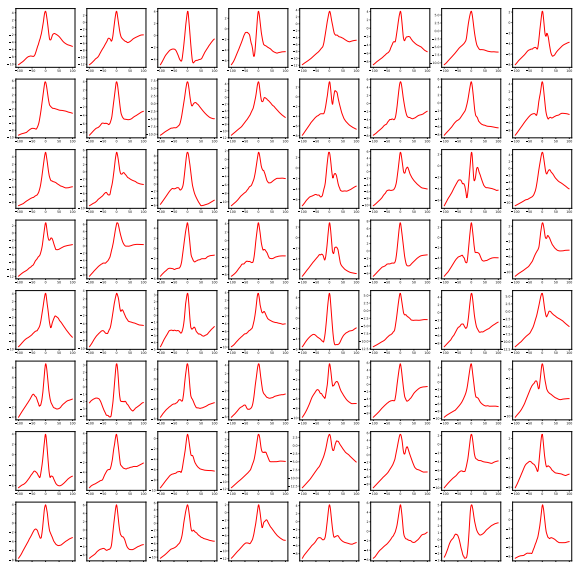
(a) Real



(b) Landscape 5000



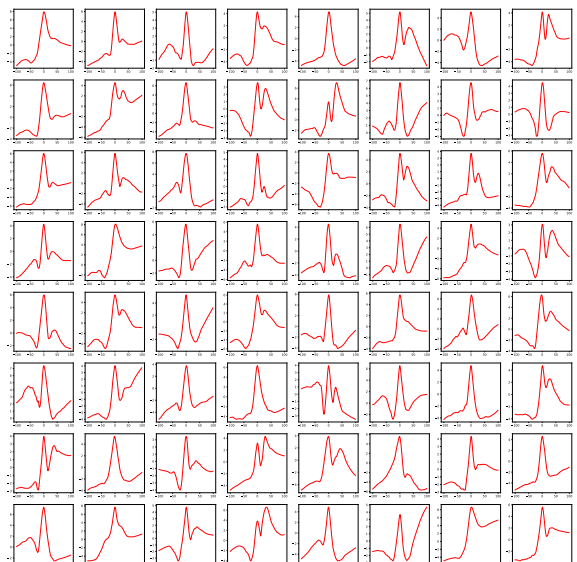
(c) Generated 50000



(d) Landscape 50000



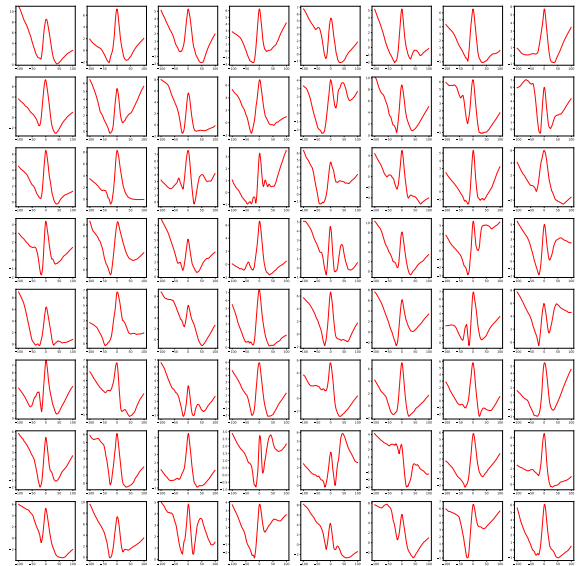
(e) Generated 100000



(f) Landscape 100000



(g) Generated 200000

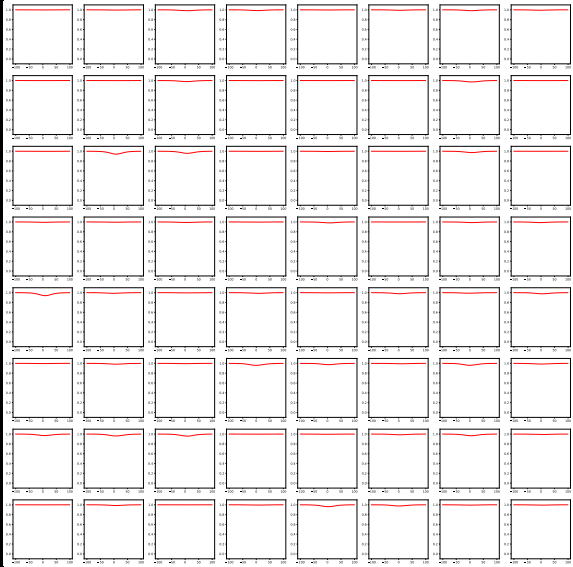


(h) Landscape 200000

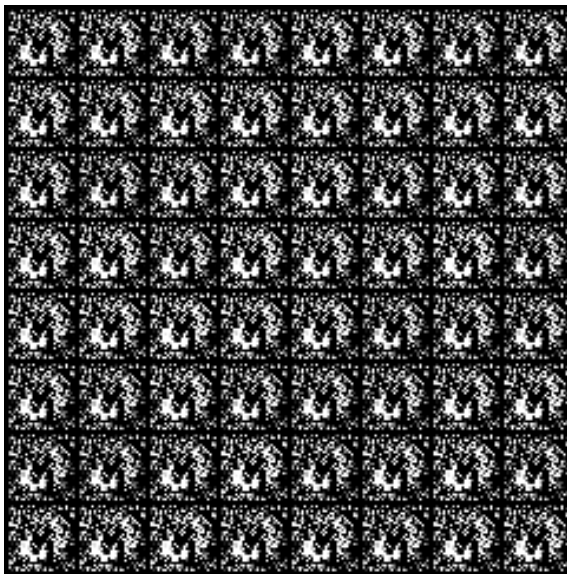
Figure 17: WGAN-GP with $\lambda = 10$



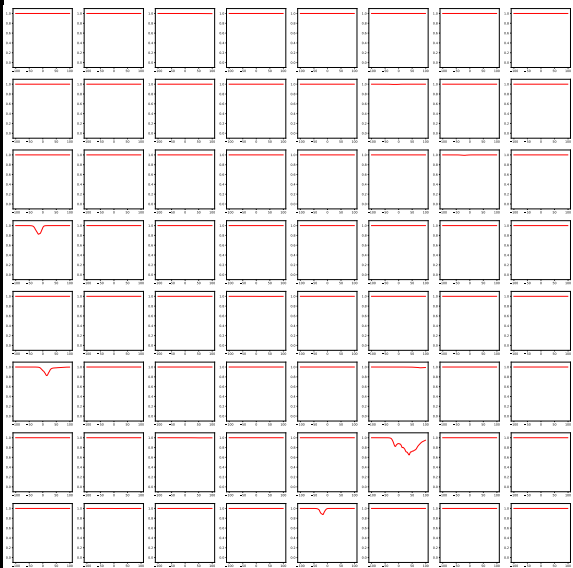
(a) Real



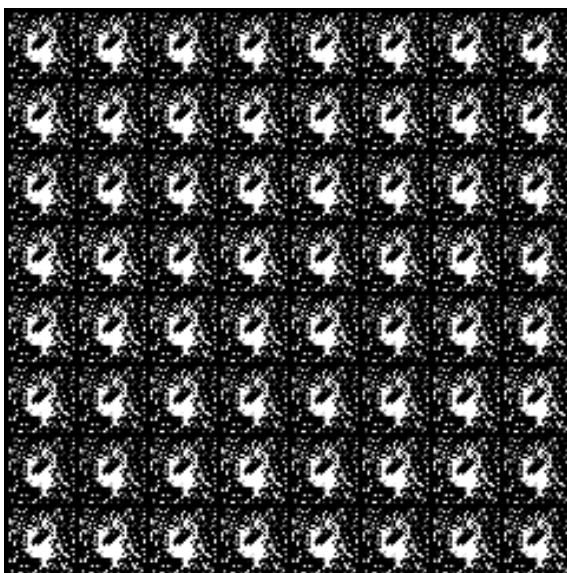
(b) Landscape 5000



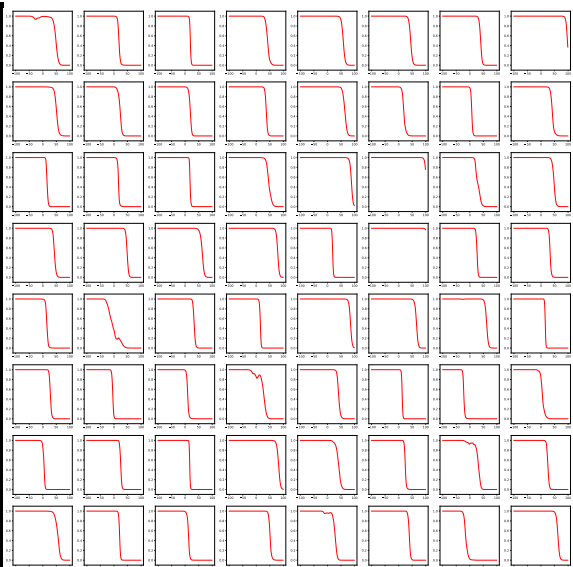
(c) Generated 50000



(d) Landscape 50000



(e) Generated 100000



(f) Landscape 50000

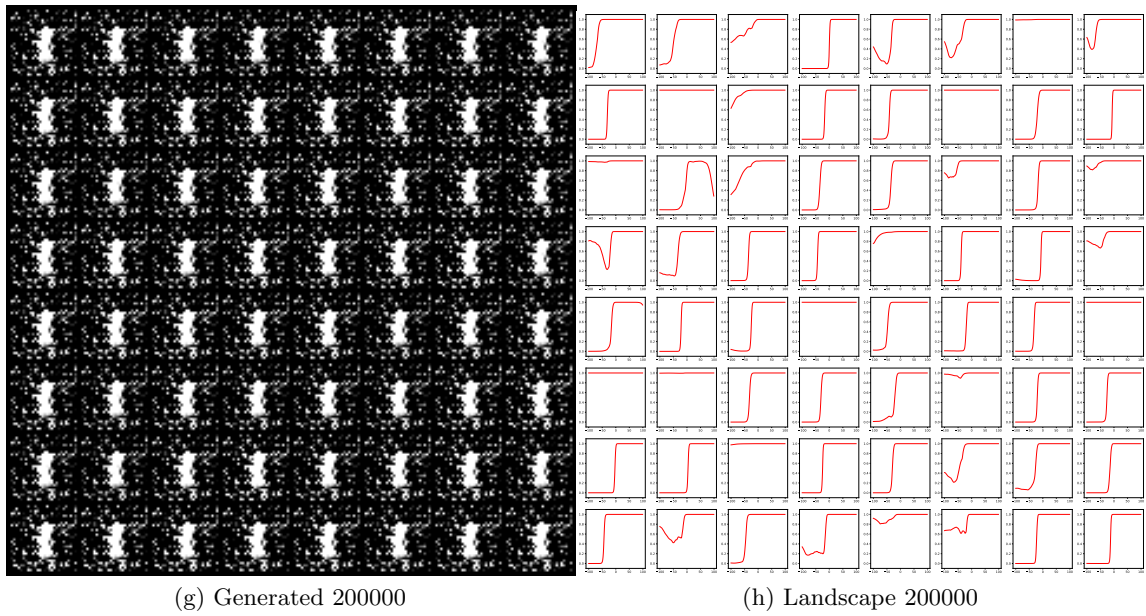


Figure 18: GAN-NS with SGD optimizer. The generator keep moving between regions of the data space and does not converge.